Advances in Polarization Based Liquid Crystal Optical Filters

Xiaowei Xia, Jay E. Stockley, Teresa K. Ewing, Steven A. Serati

Boulder Nonlinear Systems, Inc. 450 Courtney Way, Unit 107, Lafayette, CO 80026

ABSTRACT

Liquid crystal tunable filters are gaining wide acceptance in such diverse areas as optical fiber communications, astronomy, remote sensing, pollution monitoring, color generation for display and medical diagnostics. The large aperture and imaging capability of liquid crystal tunable filters represent a distinct advantage over conventional dispersive spectral analysis techniques. Furthermore, benefits of liquid crystal tunable filters over acousto-optic tunable filters include low power consumption, low addressing voltage, excellent image quality and large clear aperture. We discuss polarization interference filters based on liquid crystal tuning elements. While liquid crystal tunable filters based nematic liquid crystal, using Fabry-Perot and polarization interference effects are commercially developed, only recently has the emphasis been on liquid crystal tunable filters to include current novel developments in high-speed, analog ferroelectric-liquid crystals (FLCs). Compared to nematic liquid crystal, FLC-based tunable optical filters offer fast response time and increased field-of-view.

Keywords: Liquid crystal, FLC, tunable filter, polarization interference filter, Fabry-Perot

1. INTRODUCTION

Liquid crystal tunable filters (LCTFs) are gaining wide acceptance in such diverse areas as optical fiber communications, astronomy, remote sensing, pollution monitoring, color generation for display and medical diagnostics. The large aperture and imaging capability of LCTFs represent a distinct advantage over conventional dispersive spectral analysis techniques. Furthermore, benefits of LCTFs over acousto-optic tunable filters include low power consumption, low addressing voltage, excellent image quality and large clear aperture.

LCTFs based on nematic LC, using Fabry-Perot effects have been extensively studied by groups in Bellcore,[1,2] NTT [3,4] and Tohoku University. [5,6] They are currently available from several US vendors, including Boulder Nonlinear Systems, Inc. (BNS). To obtain high-speed liquid crystal Fabry-Perot tunable filters suitable for wavelength division multiaccess optical networks, Johnson's group at the University of Colorado utilized Chiral Smectic LC (CSLC) as the cavity material to obtain microsecond switching speed. [7,8] High-speed ferroelectric liquid crystal (FLC) Fabry-Perot tunable filters were also studied by Patel *et. al.* [9]. LCTFs based on nematic LC, using polarization interference effects have been fabricated by Kopp *et. al.* for astronomical applications, [10] and by Staromlynska *et. al.* for application in remote sensing.[11] Sharp first demonstrated the feasibility of a continuously tunable Lyot filter using chiral smectic liquid crystals.[12] In this paper, we address extension of the principles involved in tuning LCTFs to include recent development of high-speed, analog ferroelectric-liquid crystals (FLCs). There are two compelling arguments for considering ferroelectric LC-based tunable optical filters over their nematic LC cousins: fast response time and increased field-of-view. Ferroelectric LC elements have tuning speeds in the 30μs-250μs range, depending on the device thickness, the material used and temperature. This is 10-100 times faster than speeds typically observed in nematic LC mixtures. Unlike nematic LC, the switching mechanism of ferroelectric LC is conducive to acceptance angles that are independent of applied field.

2. POLARIZARTION INTERFERENCE FILTERS

Both discrete and continuous tunable filters presented subsequently are based on a technique known as polarization interference. In this scheme, the wavelength dependence of polarization induced by multiple-order waveplates is manipulated to produce a wavelength dependent transmission. Polarization interference filters are typically grouped into two classes, Solc and Lyot structures. These two types of filters have competing advantages and disadvantages, and therefore a third type, the Evans split-element filter, is presented as a compromise.

2.1 Passive Filters

The Solc filter [13] consists of a series of *N* identical retarders arranged between two polarizers. Complex field amplitudes are manipulated by the period retarder structure that, when interfered at the exit polarizer, produce a spectrally replicated band-pass transmission. There are two types of Solc configurations, folded and fan. In a folded Solc filter, the optical axis of each subsequent retarder in the stack rocks back and forth at some angle (+/- α). In a fan Solc filter, the optic axis of each subsequent retarder rotates clock-wise ($1\alpha,2\alpha,3\alpha,4\alpha$ …). While throughput is high for a Solc-type filter (with only two polarizers), the finesse (number of pass-band widths in a spectral period) scales linearly with the number of retarders. Consequently, even filters of moderate finesse require a large number of components.

The structures of passive Lyot filters are based on the work of Lyot and Ohmann. [14] These filters are made up of a cascade of filter units, or stages, requiring two linear polarizers (parallel or crossed) bounding a linear multiple-order retarder oriented at 45°. The top of Figure 1 shows a typical stage consisting of polarizer, retarder and polarizer. The filter stage functions as a two-beam (Michelson) interferometer, based on polarization rather than wavefront shearing. The transmission of a single stage, like a Michelson interferometer, is an oscillatory function of the path-length-difference. As shown in Figure 1, the thicker the retarder, the narrower the pass bands. By cascading a series of these filter stages, a bandpass filter can be synthesized. Figure 1 also shows the characteristic replicated *sinc* function transmission of a classic Lyot style filter. Note that the spectrum is produced by a geometric relationship (*d, 2d, 4d, 8d)* of retarder thickness in subsequent stages.

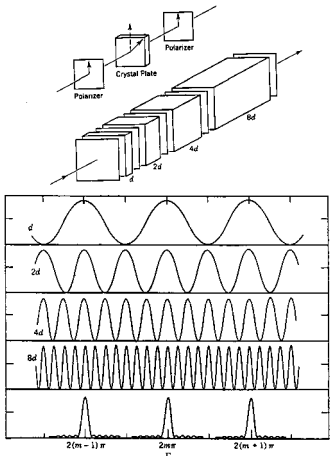

Fig. 1: A classic four-stage Lyot-Ohmann polarization interference filter (PIF) and its characteristic transmission spectrum. [15]

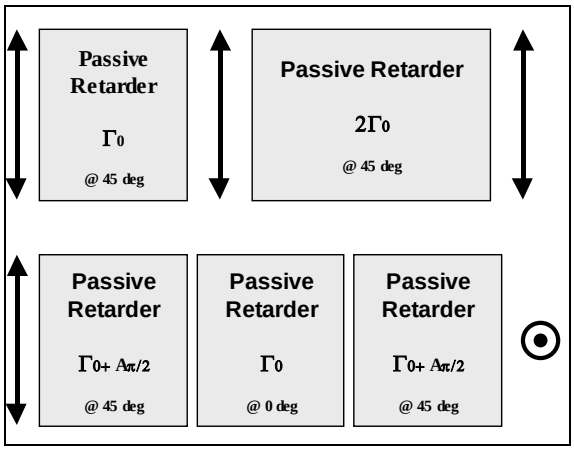

Fig. 2: A two-stage passive Lyot filter (top) and its Evans replacement (bottom).

A Solc filter offers high peak transmission, as it only uses two polarizers, but is complicated by the linear relationship between the number of retarders and the filter finesse. Conversely, the finesse of a Lyot filter increases geometric with the number of retarders, but at the cost of additional polarizers, which reduce the peak transmission of the device. A compromise solution with the most promise is the split-element filter developed by Evans.[16]

Evans introduced the split-element filter as a means of reducing the required number of polarizers in Lyot band-pass filters. A passive, single-stage split-element filter is best compared to a passive two-stage Lyot, as in Figure 2. In the equivalent split-element stage, the high order retarder is divided in half and placed on either side of the low order retarder. In order for the split-element to provide a transmission function identical to the two-stage Lyot filter, the split-elements are parallel and oriented at 45°. The central retarder is oriented parallel to the input polarization, and the exit polarizer is crossed with the input polarizer. Finally, an additional quarter-wave of retardation is required in each split-element in order to obtain the Lyot spectrum. Figure 3 shows the relationship between filter finesse and the number of

polarizers required for each of the three types of filters. Likewise, Figure 4 shows the relationship between the number of retarders needed and the filter finesse.

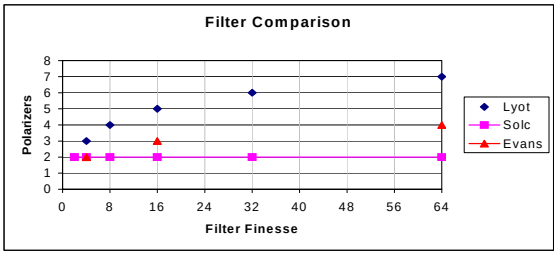

Fig. 3: Number of polarizer required for various PIF structures. polarization interference effects.

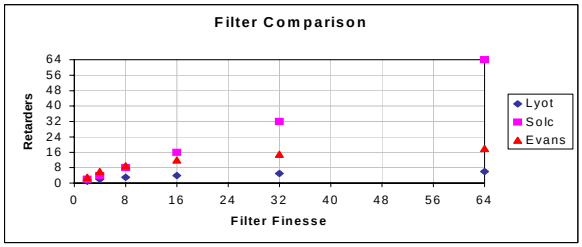

Fig. 4: Number of retarders required for various PIF structures.

2.2 Discretely Tunable Filters

Tuning the wavelength of peak transmission in the Lyot polarization interference filter (PIF) requires changing the path-length difference, or retardance, of each filter stage. This is precisely how PIFs are tuned using homogeneously aligned nematic liquid crystal.[10,11] Application of an electric field in a nematic device produces an analog variable retardation. It is therefore quite obvious how a passive PIF can be retrofitted to be active with nematic LC. Conversely, the electro-optic response of a homogeneously aligned FLC device functions as a fixed retarder with variable orientation. The mechanism for tuning a PIF is therefore not obvious. However, SmC* FLC cells can be made to function as two-state binary variable retarders. Figure 5 shows, a two-state SmC* FLC device, cascaded with a passive linear retarder functions as a binary variable retarder. With 22.5° tilt materials, the FLC is oriented parallel/perpendicular to the input polarization in the off-state, with no effect on the transmitted spectrum. In the on-state, the FLC optic axis is parallel/perpendicular to that of the multi-order passive retarder. This sum/difference retardance shifts the center wavelength of the transmitted spectrum. Using this method and multiple Lyot stages, a number of discrete wavelength shifts can be generated. In many instances this quasi-continuous tuning is sufficient and can be implemented more simply than true analog tuning.

$$T = \left\{ \cos^2\left(\frac{\Gamma_0}{2} \right) \right. \qquad \text{OFF}$$

$$T = \left\{ \cos^2\left(\frac{\Gamma_0 + \Gamma_{FLC}}{2} \right) \right. \qquad \text{ON}$$

$$T = \left\{ \cos^2\left(\frac{\Gamma_0 - \Gamma_{FLC}}{2} \right) \right. \qquad \text{OFF}$$

$$T = \left\{ \cos^2\left(\frac{\Gamma_0 + \Gamma_{FLC}}{2} \right) \right. \qquad \text{ON}$$

Fig. 5: A two-state tunable filter using 22.5° tilt FLC material (top) or 45° tilt FLC material (bottom).

Multi-state discrete switching can also be accomplished using 45° tilt FLC materials, as shown in Figure 5 (bottom). There are some significant benefits to using these materials for tuning filters. First, unlike the filters made with 22.5° tilt materials, 45° tilt FLC used in a multi-stage filter containing *m* devices produce 2^m unique states. Secondly, since the active retarder made with 45° tilt material shifts the spectrum in both states (either positive or negative), it can accomplish the same total spectral shift as a 22.5° tilt material, but at half the retardance, and therefore half the thickness. This can become quite valuable in the IR, where the devices can otherwise become quite thick.

The actual number of devices required to discretely tune a Lyot filter depends on the number of wavelength bands, the required location of the center wavelengths and the wavelength operating band (Free-spectral-range (FSR)). The latter is a consequence of the chromatic nature of the tuning elements, both for nematic and FLC tunable filters. A requirement of a large tuning range is equivalent to requiring that the active retarders function quasi-achromatically throughout the FSR. For example, tuning a filter by FSR/2 requires a half-wave shift is the lowest order stage, followed by a full-wave, two-waves, four-waves, eight-waves of shift and so on in the highest order stages. By neglecting multiple full-wave retardance shifts, the filter does not strictly maintain the geometric Lyot relationship. However, for operation over narrow FSRs, the additional stray light incurred by peak/null misalignment can be quite small.

2.3 Continuously tunable filters

Feasibility for producing a high-speed broadband continuously tunable PIF is the product of a great deal of research, in diverse areas of polarization optics. This includes not only Lyot and Ohmann's original work, but also the development of rotative tuning schemes, achromatic elements, methods for reducing the required number of polarizers, and of course, chiral smectic liquid crystal development. These significant developments have made PIF tunability using homogeneously aligned FLC devices possible.[12]

The method for obtaining continuous tunability using rotative retarders is achieved by bounding a rotative half-wave retarder by quarter-wave retarders to form a variable retarder (QHQ).[17] The tuning mechanism of the QHQ structure is very straightforward. The input light passes through a linear polarizer followed by a multi-order retarder, oriented at 45°. The retarder induces a wavelength dependent phase shift between orthogonal, equal amplitude field components manifested in a wavelength dependent polarization ellipticity. An achromatic quarter-wave retarder (oriented parallel to the input polarizer) analyzes this ellipticity, producing linear polarizations with wavelength dependent output angles. Thus the orientation of the exit polarizer determines the wavelength of peak transmission. Rotating this polarizer through 180° scans the filter through a full FSR. In practice, mechanical rotation of an exit polarizer is slow and impractical. A practical alternative is the addition of a rotating achromatic half-wave retarder preceding a fixed exit polarizer. The tunable half-wave retarder selects the desired wavelength and aligns its linear polarization output with the exit polarizer.

Electronically controlled variable retardation can be achieved using an FLC device bounded by passive quarter wave retarders. A Lyot PIF stage is tuned by cascading this zero-order active retarder with a multi-order passive retarder. Since a retarder oriented parallel to a linear polarizer has no effect on the transmitted spectrum, one of the quarter wave retarders can be omitted. The resulting tunable stage is shown in Figure 6. This analog tuner stage minimizes the number of active devices required to achieve a FSR of tuning, while simultaneously enhancing the optical tuning bandwidth through chromatic compensation.

Fig. 6: A single element continuous FLC tuner

Fig. 7: A dual element continuous FLC tuner.

Tuning each filter stage through it's respective FSR requires analog rotation of the achromatic half-wave retarder by 90° (from -45° to + 45°). For narrow FSR filters, achromatic operation of the tuning elements is achieved with zero-order retarders. Analog tunability is realized quite simply by using a homogeneously aligned SmA* device as the rotative half-wave retarder. Near ideal operation of such a filter can be achieved over bands less than 100nm in the visible, where an FLC retarder functions quasi-achromatically.

To date, a full FSR of analog tunability with a single FLC device has been limited by the inadequacy of available SmA* materials. Furthermore, zero-order retarders are not sufficiently achromatic for tunability over broad bands. One of the effects of tuner chromaticity is the reduction in rotary efficiency, at the expense of an increased ellipticity. A consequence of this fact is that a rotation of 90° is inadequate to tune the filter through a FSR at all wavelengths. Therefore, narrow gaps in the tunable ranges appear, unless a rotation exceeding 90° is used.

The continuous dual-element tuner, shown in Figure 7, utilizes two FLC active retarders to both achieve a FSR of tunability and to compensate for chromatic effects in broadband filters.

2.4 Field-of-view of polarization interference filters

Filters, such as Fabry-Perot resonators, thin-film interference filters and polarization interference filters all exhibit limited acceptance angles. This is because the spectral pass-band is shifted, due to the change in optical path length for light off-normal. For isotropic filters, the absolute optical path length in a particular layer depends upon the angle of incidence, while it is the path length difference between ordinary and extraordinary waves that is angle dependent in a PIF.

The field-of-view (FOV) of a filter is specified as corresponding to a tolerable percentage shift of a passband. The spectral shift for an isotropic thin-film filter is given by:

$$\Delta\lambda = -\frac{\lambda_0 \sin^2\theta}{2\bar{n}^2}$$

Where *n* is the index of refraction in a particular filter layer, θ is the incidence angle, and λ_0 is the design wavelength at normal incidence. Though simple, this equation illustrates several important facts. First, the spectral shift is independent of the thickness of the layer, or the resolution of the filter. Consequently, a high-resolution filter will show a much larger percentage spectral shift with incidence angle than a low-resolution filter. Second, the filter passband is, in general, blue shifted with non-normal incidence due to the reduction in retardance. Third, high-index layers can be used to improve the acceptance angle of the filter. Finally, the acceptance angle of isotropic thin film filters is independent of azimuth angle. This fact is especially important when compared thin-film filters to PIFs.

In a PIF, the phase difference between ordinary and extraordinary waves in a retarder plate is dependent upon the angle of incidence. The spectral shift in a simple Lyot filter is given by

$$\Delta\lambda = -\frac{\lambda_0 \sin^2\theta}{2\bar{n}^2}\left(1 - 2\cos^2\phi\right)$$

where ϕ is the azimuth angle with respect to the optic axis. Clearly, there is a strong dependence of spectral shift on azimuth angle, unlike the isotropic filter. For a filter that must accept a cone of light, the worst case azimuth angle is used to specify the FOV of a simple Lyot filter. Using the angles ϕ = 0°, 90°, the FOV is found to be identical in magnitude to that of an isotropic filter. However, the spectrum is either red-shifted or blue-shifted depending on whether the "sees" the fast axis or not. Furthermore, the spectral shift vanishes for the case ϕ = +/- 45°. Unlike a filter tuned with a nematic LC device, in an FLC-based Lyot PIF, the spectral shift remains constant, independent of electric field and molecular orientation.

Fig. illustrates the transmission spectra for a simple Lyot filter stage (centered at 540 nm) at various angles of incidence (0°, 15°, 30°) and worst case azimuth angle. Of course, these shifts are also representative of shifts occurring with Fabry-Perot and thin film interference filters.

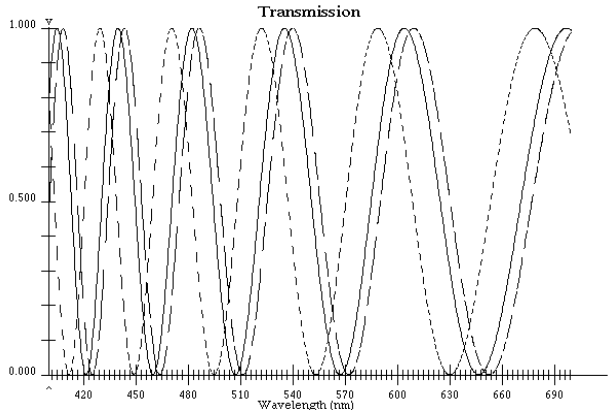

Fig. 8: Spectral shift in a Lyot PIF due to off axis incident light of 0°(red), 15°(green) and 30°(blue).

While the FOV of a Lyot PIF is quite large for particular azimuth angles, it is desirable to produce a filter with a large acceptance angle for all azimuth angles. This process is termed "wide-fielding", and is a feature exclusive to PIFs. The feasibility for wide-fielding a retarder is contingent upon the availability of a half-wave retarder (or rotator) which is achromatic over the spectral band of operation. A broadband PIF may require an element that is achromatic over a bandwidth of 300-400nm in the visible. Wide-fielding is achieved by exploiting the azimuthal dependence of the retardation shift with angle off-normal. In a Lyot filter, splitting the multi-order retarder and crossing the optic axes produces a wide-field element. The basic principle is that that a change in retardation accumulated by half of the retarder due to off-axis light is accumulated with opposite sign by the other half.

3. HIGH-SPEED ANALOG FLC MODULATORS

Development of high-speed, analog liquid crystal modulators are essential for further development of liquid crystal optical filters. To this end, analog switching FLC devices were fabricated and their usefulness as filter tuning elements was evaluated. This section highlights a proof-of-principle demonstration of a polarization interference filter (PIF) tuned using an analog switching ferroelectric liquid crystal retarder.

Polarization interference filters (PIFs) designed and fabricated by BNS prior to this effort required three active retarders per Lyot stage to continuously tune through one free spectral range (FSR). Due to the requirement of so many active retarders, the overall filter throughput suffered. During the Phase I effort, high tilt analog switching ferroelectric liquid crystals (FLCs) were investigated. To demonstrate the feasibility of replacing three active tuning elements with a single high tilt analog switching FLC, we constructed a single stage of the tunable analog FLC Lyot-type filter. The filter stage consisted of a 4-wave passive retarder centered at 600 nm, an achromatic quarter-wave retarder, and a high-tilt analog switching FLC half-wave retarder (with a design wavelength of 574 nm), sandwiched between parallel polarizers.

Fig. shows examples of the normalized output spectrum measured for the tunable Lyot stage while various voltages were applied to the analog switching FLC. The spectra were obtained using an optical spectrum analyzer. The transmission spectra shown in Fig. consist of two nulls. With no voltage applied to the analog FLC retarder, one null is in the green, the other at the long end of the red. Each of these nulls blue-shifts with applied voltage, that is that the green null shifts to blue and the red null shifts to green. The filter tunes through one FSR in the green using a single active FLC device.

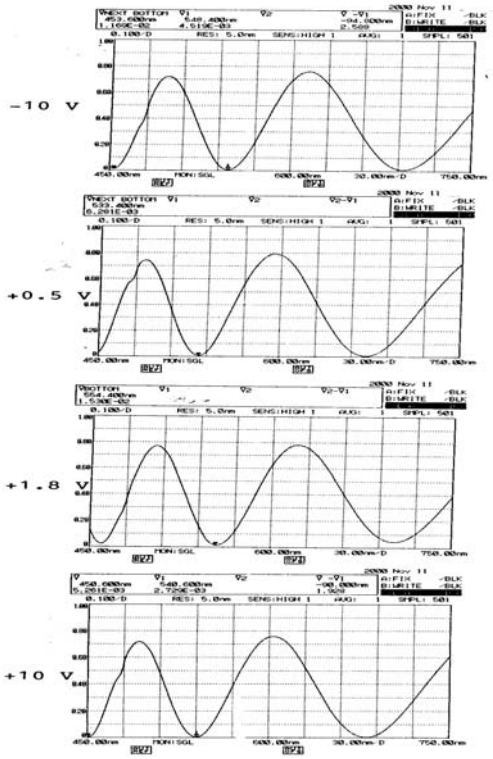

Fig. 9: Experimental spectra for various voltages applied to a high-tilt analog FLC used to tune a single stage Lyot filter.

Table 1 gives the voltage dependence of the two null wavelengths, as measured in the proof-of-principle device. Measurement error is ± 2 nm.

Applied Voltage	Green to Blue Null Shift	Red to Green Null Shift
-10 V	548 nm	695 nm
0 V	537 nm	676 nm
0.5 V	533 nm	670 nm
1.0 V	529 nm	665 nm
1.5 V	513 nm	630 nm
1.8 V	461 nm	554 nm
3.0 V	454 nm	549 nm
10 V	450 nm	540 nm

Table 1. Null shift as a function of voltage for the single stage tunable Lyot filter implemented using analog switching FLC.

This prototype filter was not optimized and there is a reduced contrast (from over 100:1 at the extremes to 10:1 in the mid-ranges). This is in part due to the imperfect switching characteristics exhibited by the analog switching FLC (out of plane director switching) and the chromaticity of the waveplate. In addition, Fresnel losses from the elements of the filter stage limited the transmission to about 82% in the visible. This can be improved using antireflection coatings.

Improvements to the analog switching FLC and optimization of the filter design are slated for the future effort. One of the goals is to implement a visible tunable filter exhibiting 1000:1 contrast ratio. The implementation will also take advantage of the increased throughput of the Evans split-element design.

4. CONCLUSION

We have reviewed the advances in Polarization Based Liquid Crystal Optical Filters. Various kinds of polarization interference filters were discussed. Development of high-speed, analog liquid crystal modulators are essential for further development of liquid crystal optical filters. We have therefore fabricated analog switching FLC devices and evaluated their usefulness as filter tuning elements. We performed a proof-of-principle demonstration of a polarization interference filter (PIF) tuned using an analog switching ferroelectric liquid crystal retarder. Our goal is to fabricate a high-speed tunable notch filter that is easy to fabricate, low-cost and flexible enough to address the needs of many diverse applications. These goals place a large demand on the ferroelectric LC material itself.

ACKNOWLEDGMENTS

This research was funded through Air Force Contract F33615-01-C-5406 by Wight-Patterson Air Force Research Laboratory. Boulder Nonlinear Systems is indebted to the past research of Gary Sharp which formed the foundation for the work discussed here. Finally, the authors are grateful to L.C. Chien of the Liquid Crystal Institute at Kent State University for the helpful discussions on new material developments in ferroelectric liquid crystals.

REFERENCES

1. J. S. Patel, M. A. Saifi, D. W. Berreman, Chinlon Lin, N. Andreadakis and S. D. Lee, "Electrically tunable optical filter for infrared wavelength using liquid crystals in a Fabry-Perot etalon," *Appl. Phys. Lett.* **57**, pp.1718-1720, 1990.

2. J. S. Patel and M. W. Maeda, "Tunable polarization diversity liquid-crystal wavelength filter," *IEEE Photon. Technol. Lett.* **3**, pp.739-740, 1991.

3. K. Hirabayashi, H. Tsuda and T. Kurokawa, "Narrow-band tunable wavelength-selective filters of Fabry-Perot interferometer with a liquid crystal intracavity," *IEEE Photon. Technol. Lett.* **3**, pp.213-215, 1991.

4. S. Matsumoto, K. Hirabayashi, S. Sakata and T. Hayashi, "Tunable wavelength filter using nano-sized droplets of liquid crystal," *IEEE Photon. Technol. Lett.* **11**, p.442, 1999.

5. H. Yoda, Y. Ohtera, O. Hanaizumi, S. Kawakami, "Analysis of polarization-insensitive tunable optical filter using liquid crystal: connection formula and apparent paradox," *Opt. and Quantum. Electron.* **29**, pp.285-299, 1997.

6. Y. Ohtera, H. Yoda and S. Kawakami, "Analysis of twisted nematic liquid crystal Fabry-Perot interferometer filter (TN-FPI) based on the coupled mode theory," *Opt. and Quantum. Electron.* **32**, pp.147-167, 2000.

7. A. Sneh, K. M. Johnson and J-Y Liu, "High-speed wavelength tunable liquid crystal filter," *IEEE Photon. Technol. Lett.* **7**, pp.379-381, 1995.

8. Y. Bao, A. Sneh, K. Hsu, K. M. Johnson, J-Y Liu, C. M. Miller, Y. Monta and M. B. McClain, "High-speed liquid crystal fiber Fabry-Perot tunable filter," *IEEE Photon. Technol. Lett.* **8**, pp.1190-1192, 1996.

9. J. S. Patel, "Electricity tunable ferroelectric liquid-crystal Febry-Perot filter," *Opt. Lett.* **17**, pp456-458, 1992.

10. G. A. Kopp, M. J. Derks, D. F. Elmore, D. M. Hassler, J. C. Woods, J. L. Streete, and J. G. Blankner, "Tunable liquid-crystal filter for solar imaging at the He I 1083-nm line," *Appl. Opt.* **36**, pp.291-296, 1997.

11. J. Staromlynska, S. M. Rees, and M. P. Gillyon, "High-performance tunable filter," *Appl. Opt.* **37**, pp. 1081-1088, 1998.

12. G. D. Sharp, “Chiral smectic liquid crystal tunable optical filters and modulators,” Ph.D. dissertation, University of Colorado, Boulder, Colorado, 1992.

13. I. Solc, “Birefringent chain filters,” *J. Opt. Soc. Am.*, **55**, p.621, 1965.

14. B. Lyot, “Optical apparatus with wide-field using interference of polarized light,” *C.R. Acad. Sci., Paris*, **197**, p.1593, 1933.

15. Pochi Yeh, *Optical Waves in Layered Media*, p. 254, John Wiley & Sons, Inc., New York, 1988.

16. J. Evans, “The birefringent filter,” *J. Opt. Soc. Amer*., **39**, p. 229, 1949.

17. R. Clark Jones, “A new calculus for the treatment of optical systems III,” *J. Opt. Soc. Amer.*, **31**, p.500, 1941.